Monthly Notices
of the
ROYAL ASTRONOMICAL SOCIETY
MNRAS **457,** 3732–3742 (2016) doi:10.1093/mnras/stw198

State-to-state vibrational kinetics of H_2 and H_2^+ in a post-shock cooling gas with primordial composition

C. M. Coppola,[1,2,3★] G. Mizzi,[4,5] D. Bruno,[6] F. Esposito,[6] D. Galli,[2★] F. Palla[2] and S. Longo[1,2,6★]

[1]*Dipartimento di Chimica, Università degli Studi di Bari, Via Orabona 4, I-70126 Bari, Italy*
[2]*INAF – Osservatorio Astrofisico di Arcetri, Largo E. Fermi 5, I-50125 Firenze, Italy*
[3]*Department of Physics and Astronomy, University College London, Gower Street, London WC1E 6BT, UK*
[4]*Centre for Complexity Science, Zeeman Building, University of Warwick, Coventry CV4 7AL, UK*
[5]*Dipartimento di Fisica, Università degli Studi di Bari, Via Orabona 4, I-70126 Bari, Italy*
[6]*Nanotec-CNR, Section of Bari, via Amendola 122/D, I-70126 Bari, Italy*

Accepted 2016 January 21. Received 2016 January 21; in original form 2015 January 9

ABSTRACT

The radiative cooling of shocked gas with primordial chemical composition is an important process relevant to the formation of the first stars and structures, as well as taking place also in high-velocity cloud collisions and supernovae explosions. Among the different processes that need to be considered, the formation kinetics and cooling of molecular hydrogen are of prime interest, since they provide the only way to lower the gas temperature to values well below $\sim 10^4$ K. In previous works, the internal energy level structure of H_2 and its cation has been treated in the approximation of ro-vibrational ground state at low densities, or trying to describe the dynamics using some arbitrary $v > 0$ H_2 level that is considered representative of the excited vibrational manifold. In this study, we compute the vibrationally resolved kinetics for the time-dependent chemical and thermal evolution of the post-shock gas in a medium of primordial composition. The calculated non-equilibrium distributions are used to evaluate effects on the cooling function of the gas and on the cooling time. Finally, we discuss the dependence of the results to different initial values of the shock velocity and redshift.

Key words: molecular processes – shock waves – early Universe.

1 INTRODUCTION

Shock waves are commonly found in astrophysical processes involving first structure formation, either galaxies or during the gravitational collapse of the first stars. It is then interesting to investigate the detailed microphysics for a gas of primordial composition. In fact, in a shocked gas the cooling sensitively depends on the radiative transitions of the chemical components and their rapidly changing abundances. Atomic hydrogen and helium are very inefficient at radiatively cooling below $\sim 10^4$ K because in a gas in collisional equilibrium they are usually completely recombined. The lack of electrons and the cut-off in the functional dependence of the Ly α excitation rate on temperature are responsible for the steep drop of the cooling function in this temperature regime. However, after the gas is shocked at temperatures far above 10^4 K, cooling proceeds faster than recombination, leaving an enhanced ionization fraction that promotes the formation of molecular hydrogen through the intermediaries H^- and H_2^+. Furthermore, the presence of H_2 makes possible further radiative cooling down to $\sim 10^2$ K by ro-vibrational line excitation, as discussed by e.g. Shapiro & Kang (1987) and Machida et al. (2005).

In this paper, we consider the case of a strong, stationary and ionizing shock, as expected from a supernova explosion or during the virialization of a primordial density perturbation (e.g. Takizawa & Mineshige 1998; Birnboim, Keshet & Hernquist 2010). The novelty of our approach is that the network of vibrationally resolved chemical processes involving H_2 and H_2^+ in the post-shock region is included in the kinetics, following the method described by Coppola et al. (2011a). Prior to this study, the problem has been studied under various assumptions concerning the internal level distribution of H_2; for example, Shapiro & Kang (1987) tried to model vibrational excitation inserting a representative excited level (more specifically, $v = 6$), while Johnson & Bromm (2006) used the ground state approximation. This hypothesis was justified by the consideration that the collision time between atomic and molecular hydrogen is far longer than the decay time of the vibrational levels so that the excited levels are radiatively depopulated. However, it has been shown by Coppola et al. (2011a) that a non-equilibrium distribution

★ E-mail: carla.coppola@uniba.it (CMC); galli@arcetri.astro.it (DG); savino.longo@nanotec.cnr.it (SL)

can arise because of the specific features of the chemical formation pathway. For example, during the recombination process, the formation of H_2 proceeds via the highest excited levels. The resulting non-equilibrium distribution function can then be used as the actual level population at each time step to yield a more realistic description of the cooling of the gas.

The paper is organized as follows: in Section 2 the equations and approximations used are described, both for the dynamical and chemical model together with the adopted cooling and heating functions. In Section 3 the results obtained using different initial conditions are presented and the calculated non-equilibrium distributions are described and explained in the light of the detailed chemical processes.

2 FORMULATION OF THE PROBLEM

2.1 Jump conditions

In our study, we consider shocks in a gas of primordial composition. Thus, the gas mixture of the pre-shocked phase consists of H, He and D nuclei with an abundance defined by the current cosmological models. The Rankine–Hugoniot jump conditions are derived assuming the conservation of mass, momentum and energy between the pre- and post-shock regions. Hereafter, each quantity related to the pre- and post-shock is denoted with the subscript '1' and '2', respectively. We assume that in the pre-shock phase the gas is composed only by H, He and D atoms, with number density

$$n_1 = n_{1,\mathrm{H}} + n_{1,\mathrm{D}} + n_{1,\mathrm{He}}, \tag{1}$$

and that the temperature is low enough that internal atomic excitation can be neglected. These initial conditions are appropriate for most of the redshift interval from the recombination to the epoch of formation of the first structures. In the following, the ratios between the initial fractional abundance of H, He and D will be expressed by the symbols x_{H}, x_{He} and x_{D}, respectively. The numerical values adopted are $x_{\mathrm{H}} = 0.924$, $x_{\mathrm{He}} = 0.07599$, $[\mathrm{D/H}] = 2.6 \times 10^{-5}$. They have been obtained in the Λ cold dark matter cosmological model with implemented cosmological parameters according to Planck Collaboration XIII (2015).

Behind the shock the gas density can be written as

$$n_2 = n_{2,\mathrm{H}} + n_{2,\mathrm{He}} + n_{2,\mathrm{D}} + n_{2,\mathrm{H}^+} + n_{2,\mathrm{He}^{++}} + n_{2,\mathrm{He}^+} + n_{2,\mathrm{D}^+} + n_{2,\mathrm{e}^-}. \tag{2}$$

Defining the ionization degrees of H, He, He^+ and D as α_1, α_2, α_3 and α_4, the corresponding Saha equations can be written as

$$n_{\mathrm{e}} \frac{\alpha_1}{1-\alpha_1} = \frac{2\,g(\mathrm{H}^+)}{g(\mathrm{H})} n_0 \cdot \mathrm{e}^{-\frac{I_{\mathrm{H}}}{k_{\mathrm{B}} T_2}}, \tag{3}$$

$$n_{\mathrm{e}} \frac{\alpha_2(1-\alpha_3)}{1-\alpha_2} = \frac{2\,g(\mathrm{He}^+)}{g(\mathrm{He})} n_0 \cdot \mathrm{e}^{-\frac{I_{\mathrm{He}}}{k_{\mathrm{B}} T_2}}, \tag{4}$$

$$n_{\mathrm{e}} \frac{\alpha_3}{1-\alpha_3} = \frac{2\,g(\mathrm{He}^{++})}{g(\mathrm{He}^+)} n_0 \cdot \mathrm{e}^{-\frac{I_{\mathrm{He}^+}}{k_{\mathrm{B}} T_2}}, \tag{5}$$

$$n_{\mathrm{e}} \frac{\alpha_4}{1-\alpha_4} = \frac{2\,g(\mathrm{D}^+)}{g(\mathrm{D})} n_0 \cdot \mathrm{e}^{-\frac{I_{\mathrm{D}}}{k_{\mathrm{B}} T_2}}, \tag{6}$$

where

$$n_0 \equiv \left(\frac{2\pi m_{\mathrm{e}} k_{\mathrm{B}} T_2}{h^2} \right)^{3/2}. \tag{7}$$

Here, g represents the degeneracy of the nucleus and n_{e} is the total electron density deriving from all the ionization processes. These equations must be solved along with mass, momentum and energy conservation

$$\rho_1 v_1 = \rho_2 v_2, \tag{8}$$

$$p_1 + \rho_1 v_1^2 = p_2 + \rho_2 v_2^2, \tag{9}$$

$$h_1 + \frac{v_1^2}{2} = h_2 + \frac{v_2^2}{2}. \tag{10}$$

Here, v is the gas velocity, ρ_1 and ρ_2 are the mass densities before and after the shock,

$$\rho_1 = n_{1,\mathrm{H}} m_{\mathrm{H}} + n_{1,\mathrm{He}} m_{\mathrm{He}} + n_{1,\mathrm{D}} m_{\mathrm{D}} \equiv n_1 m_1, \tag{11}$$

with

$$m_1 = x_{\mathrm{H}} m_{\mathrm{H}} + x_{\mathrm{D}} m_{\mathrm{D}} + x_{\mathrm{He}} m_{\mathrm{He}}, \tag{12}$$

and

$$\rho_2 = n_{2,\mathrm{H}^+} m_{\mathrm{H}^+} + n_{2,\mathrm{He}^+} m_{\mathrm{He}^+} + n_{2,\mathrm{He}^{++}} m_{\mathrm{He}^{++}} + n_{2,\mathrm{D}^+} m_{\mathrm{D}^+} + n_{2,\mathrm{e}^-} m_{\mathrm{e}^-}, \tag{13}$$

and p is the gas pressure given by the ideal gas law

$$p_i = n_i k_{\mathrm{B}} T_i, \qquad i = 1, 2. \tag{14}$$

Finally, the enthalpy per unit mass h is defined as

$$h_1 = \frac{5}{2} \left(\frac{n_1 k_{\mathrm{B}} T_1}{\rho_1} \right), \tag{15}$$

$$h_2 = \frac{5}{2} \left(\frac{n_2 k_{\mathrm{B}} T_2}{\rho_2} \right) + \frac{n_{2,\mathrm{H}^+} I_{\mathrm{H}} + n_{2,\mathrm{D}^+} I_{\mathrm{D}} + n_{2,\mathrm{He}^+} I_{\mathrm{He}} + n_{2,\mathrm{He}^{++}} I_{\mathrm{He}^+}}{\rho_2}, \tag{16}$$

where I_{H}, I_{D}, I_{He} and I_{He^+} are the ionization potentials of H, D, He and He^+.

Defining $x \equiv \rho_2/\rho_1$ as the compression ratio and combining the equations for the conservation of momentum and energy, the relationship between the pre- and post-shock densities becomes

$$4 v_1^2 x^{-2} - 5 \left(v_1^2 + \frac{k_{\mathrm{B}} T_1}{m_1} \right) x^{-1} + v_1^2 + \frac{5 k_{\mathrm{B}} T_1}{m_1} - 2I = 0, \tag{17}$$

where the term I takes into account the energy used for the ionization of H, D and He in the shock front,

$$I = \frac{x_{2\mathrm{H}^+} I_{\mathrm{H}}}{m_2} + \frac{x_{2\mathrm{D}^+} I_{\mathrm{D}}}{m_2} + \frac{x_{2\mathrm{He}^+} I_{\mathrm{He}}}{m_2} + \frac{x_{2\mathrm{He}^{++}} I_{\mathrm{He}^+}}{m_2}. \tag{18}$$

The pre-shock density of the gas is calculated at a redshift z, assuming a uniform intergalactic medium with density $n_{\mathrm{H}} \approx 0.19(1+z)^3\ \mathrm{m}^{-3}$. As an illustration, at $z = 10$, $n_{\mathrm{H}} = 250\ \mathrm{m}^{-3}$. Neglecting the trivial solution (for which the density after the shock is equal to the density before the front), we obtain for the compression ratio the value $x = 5$, close to the asymptotic value (for strong shocks $x = 4$).

2.2 Chemical network

We consider the following species: e^-, H, H^+, H^-, H_2, H_2^+, D, D^+, D^-, He, He^+, He^{++}, HD, HD^+, HeH^+, H_3^+. In the first phase of the shock the helium chemistry plays an important role and the kinetics of formation and destruction of HeH^+ has been introduced

to follow the recombination of helium cations. The rate coefficients for processes not involving molecules are listed in Table A1, while those for molecular processes (including formation, destruction and redistribution among the vibrational manifolds) have been taken from Coppola et al. (2011a, see Table A2). The ground electronic states of H_2 and H_2^+ support 15 and 19 bound vibrational levels including the vibrational ground state, respectively.

The major formation pathway for H_2^+ is the radiative association (Mihajlov et al. 2007; Ignjatović et al. 2014),

$$H^+ + H \rightarrow H_2^+ + h\nu, \tag{19}$$

while destruction is mainly achieved through dissociative recombination (Takagi 2005; Motapon et al. 2008, 2014),

$$H_2^+ + e^- \rightarrow H + H, \tag{20}$$

photodissociation (Mihajlov et al. 2007; Ignjatović et al. 2014),

$$H_2^+ + h\nu \rightarrow H + H^+, \tag{21}$$

and charge transfer (Krstic 2002; Krstic, Schultz & Janev 2002),

$$H_2^+ + H \rightarrow H_2 + H^+. \tag{22}$$

The main formation channels for H_2 include associative detachment (Cízek, Horácek & Domcke 1998; Kreckel et al. 2010)

$$H + H^- \rightarrow H_2 + e^- \tag{23}$$

and charge transfer (Krstic 2002; Krstic et al. 2002)

$$H_2^+ + H \rightarrow H_2 + H^+. \tag{24}$$

All the vibrationally resolved processes introduced are listed in Table A2 following the model by Coppola et al. (2011a) where an analysis of each process can be found. It should be noted that both collisional excitations and de-excitations for H impact and spontaneous radiative transitions have been included in the kinetic model as well as in the cooling and heating functions. For some specific channel where no state-to-state data have been found, the nascent distributions have been estimated according to the exothermicity of the process and on available information. For H_2 and H_2^+ recombination the work by Schatz, Badenhoop & Eaker (1987) has been considered to justify the formation mainly in higher vibrational levels. It is important to mention that for the chemical processes involving H_3^+ the vibrational levels of H_2 and H_2^+ have been taken equal to the highest levels since the recombination most likely proceeds in this way (e.g. Schatz et al. 1987); however, accurate state-to-state calculations would be necessary for the proper description of the chemical kinetic effects due to this channel.

To study the evolution of the chemical composition in the post-shock gas, the system of ordinary differential equations must be solved:

$$\frac{\mathrm{d}n_j}{\mathrm{d}t} = -n_j \sum_{j'} (R_{jj'} + P_{jj'} + n_{\mathrm{H}}\gamma_{jj'}) + \sum_{j'} R_{jj'} n_{j'} + \sum_{j'} \sum_{j''} \mathbf{C}_j^{j'j''} n_{j'} n_{j''}, \tag{25}$$

where the symbols have the following meaning:

(i) n_j are the densities of the various species. In this notation, different vibrational levels of H_2 and H_2^+ have a different index j;

(ii) $R_{jj'}$ are the spontaneous and stimulated excitation and de-excitation rates, that can be expressed in terms of the Einstein coefficients $A_{jj'}$ as

$$R_{jj'} = \begin{cases} A_{jj'}[1 + \eta_{jj'}(T_{\mathrm{r}})] & \text{if } j > j' \\ (g_{j'}/g_j) A_{jj'} \eta_{jj'}(T_{\mathrm{r}}) & \text{if } j < j' \end{cases}, \tag{26}$$

where the statistical weight of the molecular vibrational levels is $g_j = 1$ since there is no vibrational degeneracy and $\eta_{jj'}(T_{\mathrm{r}}) = [\exp(h\nu_{jj'}/k_{\mathrm{B}}T_{\mathrm{r}}) - 1]^{-1}$, where $T_{\mathrm{r}} = 2.73(1 + z)$ K is the temperature of the cosmic microwave background (CMB);

(iii) $P_{jj'}$ are the destruction rates of the jth species due to photons;

(iv) $\gamma_{jj'}$ are the excitation/de-excitation rate coefficients of the jth species for collision with H;

(v) $C_j^{j'j''}$ are the formation rates of the jth species for collision between the j'th and j''th species, photons included.

Since we do not resolve the molecular rotational energy levels, we have computed the Einstein coefficients for the vibrational transitions by averaging the fully resolved $A_{(v,J)\rightarrow(v',J')}$ computed by Wolniewicz, Simbotin & Dalgarno (1998) over a thermal distribution of rotational level populations. As a consequence, the $A_{vv'}$ are functions of the temperature, like the collisional rate coefficients $\gamma_{vv'}(T)$. For the latter, at high temperatures we have adopted the results obtained by Esposito & Capitelli (2009) using the quasi-classical trajectory method. It is well known that at temperatures below ∼500–600 K quantum-mechanical effects should be taken into account. Thus, we have included in the kinetics the data by Flower (1997) and Flower & Roueff (1998, 24 ortho- and 27 para-transitions) down to 100 K. All the data available for ro-vibrational transitions have been adopted averaging on the rotational distribution. At lower temperatures, data have been extrapolated using an Arrhenius-type law. Fig. 1 shows the Einstein coefficients $A_{vv'}(T)$ and the collisional rate coefficients $\gamma_{vv'}(T)$ as function of the temperature.

The full system of equations has been numerically solved. The rate coefficients for atomic processes are computed as function of the temperature of the gas for collisional processes and of the temperature of the CMB for processes involving photons. For molecular processes, the rate coefficients are computed by interpolating state-to-state calculated rate coefficients. The various contributions to the cooling function are computed from analytical expressions, that are reported in Table A3 together with the corresponding references. The fractional abundance of electrons is obtained by imposing charge neutrality. Other contributions to the cooling function due to atomic processes are listed in Table A3.

2.3 Cooling and heating

It is useful to summarize the conservation laws that hold between the pre- and post-shock quantities. Behind the shock front conservation of mass and momentum still applies

$$\rho \frac{\mathrm{d}v}{\mathrm{d}t} = -v \frac{\mathrm{d}\rho}{\mathrm{d}t}, \tag{27}$$

$$\frac{\mathrm{d}p}{\mathrm{d}t} = v^2 \frac{\mathrm{d}\rho}{\mathrm{d}t}, \tag{28}$$

where we have dropped the subscript 2 for clarity. The energy equation can be written as an equation for the evolution of temperature:

$$\frac{\mathrm{d}T}{\mathrm{d}t} = (\gamma - 1)\left(\frac{\Gamma - \Lambda}{n k_{\mathrm{B}}} + \frac{T}{n}\frac{\mathrm{d}n}{\mathrm{d}t}\right) + \gamma \frac{T}{\mu}\frac{\mathrm{d}\mu}{\mathrm{d}t}, \tag{29}$$

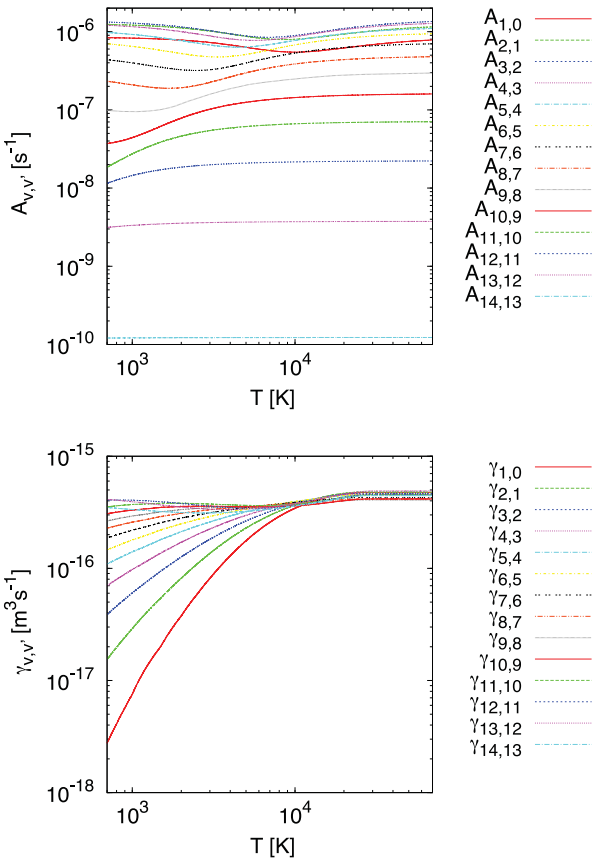

Figure 1. Evolution of state-resolved thermally averaged Einstein coefficients $A_{v,v'}$ and collisional coefficients $\gamma_{v,v'}$ as a function of T; among the full set of transitions included in the kinetic model, only the coefficients for the transitions with $\Delta v = 1$ are shown here as an example.

where μ is the mean atomic weight. We assume that γ is constant and equal to the monoatomic value $\gamma = 5/3$. This is justified by the fact that the fractional abundance of molecular hydrogen is always negligible and the gas can essentially be regarded as monoatomic.

Equation (29) can be simplified using some approximations. The last term is usually negligible since it changes primarily because of recombination. In addition we can assume that the pressure is constant. Indeed, previous work (Shapiro & Kang 1987) has shown that the pressure varies only slightly, as confirmed by our complete calculations. With these assumptions, the equation for the gas temperature can be simplified as

$$\frac{\mathrm{d}T}{\mathrm{d}t} = \frac{\gamma - 1}{\gamma}\left(\frac{\Gamma - \Lambda}{nk_{\mathrm{B}}}\right). \tag{30}$$

If $T \gg 10^4$ K a shocked gas cools faster than it recombines. Thus, recombination is not in equilibrium and there is a significant ionization fraction below 10^4 K which allows H^- and H_2^+ to form and eventually produce H_2 molecules. Even though its abundance is small, H_2 is the only possible cooling agent down to $\sim$100 K by means of ro-vibrational line excitation; for the same reasons, at lower temperatures HD allows us to cool even more efficiently (Johnson & Bromm 2006; Shchekinov & Vasiliev 2006). In these conditions the gas is completely neutral and H_2 excitation occurs only via collisions with H. Radiative cooling functions computed in the local thermodynamic equilibrium (LTE) approximation are available for some of the molecules included in the present model, namely HD^+, HeH^+ and H_3^+ (Miller et al. 2010; Coppola, Lodi & Tennyson 2011b). However, the critical densities for most of the transitions of these molecules are much higher than the density regime covered by our calculations and for this reason they have not been included.

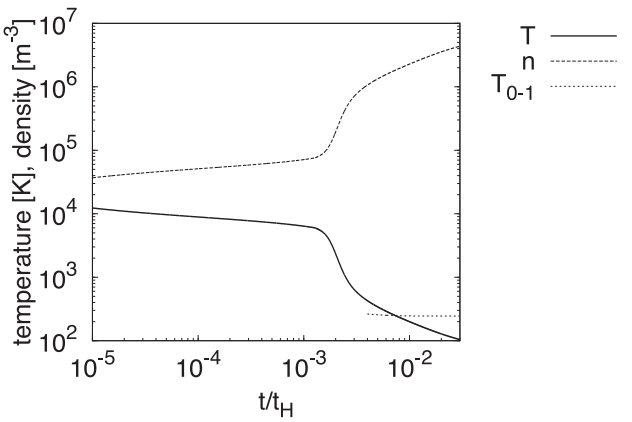

Figure 2. Temperature and density profiles as a function of time; the value of the excitation temperature of the lowest vibrational transition T_{1-0} is shown for comparison (see the comments given in Section 3).

Several cooling mechanisms have been included in the model, both involving atoms/ions and molecules. Among the former, the following processes have been inserted:

(i) radiative cooling from collisional excitation of H and He^+;
(ii) cooling by H and He collisional ionization;
(iii) bremsstrahlung;
(iv) Compton cooling;
(v) cooling by recombination of H^+, He^+ and He^{++}.

While for the latter, we have considered:

(i) cooling for the collisions: H_2/H, H_2/H_2, H_2/He, H_2/H^+ and H_2/e^-;
(ii) HD cooling.

Concerning the contribution of HD cooling, we have included the biparametric fit provided by Lipovka, Núñez López & Avila-Reese (2005). In order to extend the calculation to higher z the cooling function for HD should be corrected: in fact, the fit provided by Lipovka et al. (2005) has been calculated at $z = 0$.

Two other processes have also been included in the thermal energy balance, namely the heating due to the formation of H_2 via H^- and the cooling due to the electron attachment in the formation of the negative ion H^-. For the former, the specific reaction rates $k^{v_i}_{ass\_det}$ for each vibrational level have been used in the calculation:

$$\Gamma = \sum_{v_i} k^{v_i}_{ass\_det} n_{\mathrm{H}} n_{\mathrm{H}^-} (E_{v_i} - E_0). \tag{31}$$

The details about the implemented fits for each cooling/heating contribution and their references can be found in Table A3.

The resulting trend for gas temperature and density is shown in Fig. 2.

3 RESULTS

As a standard case, we consider here the shock produced by a supernova explosion with a shock velocity $v_s = 50$ km s^{-1} and a pre-shock hydrogen density corresponding to the baryon density at $z = 20$. For $v_s \lesssim 50$ km s^{-1}, the post-shock radiation can be neglected (Shapiro & Kang 1987). Moreover, together with the

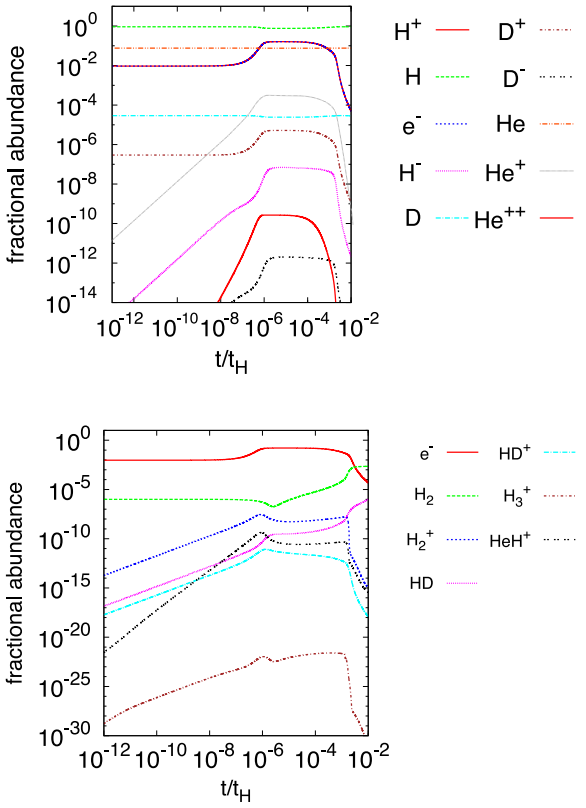

Figure 3. Fractional abundances of selected species. Top panel: atoms. Bottom panel: molecular species. For vibrationally resolved species only the abundance in the $v = 0$ level is shown.

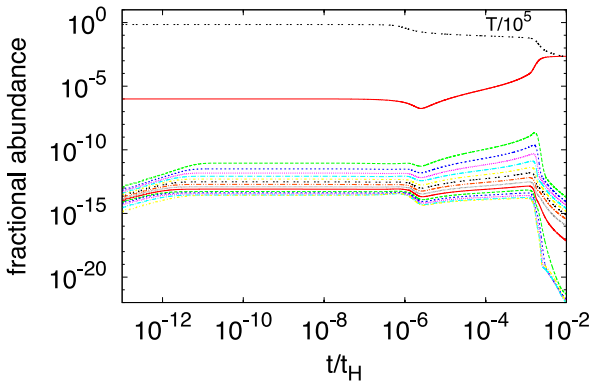

Figure 4. Fractional abundance of H_2, from $v = 14$ (bottom curve) to $v = 0$ (top curve). The gas temperature is also shown as a reference.

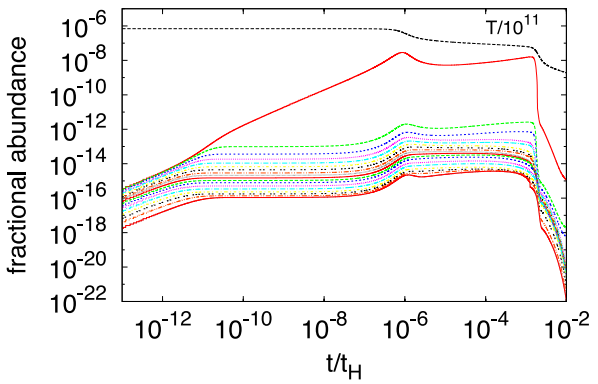

Figure 5. Fractional abundance of H_2^+, from $v = 18$ (bottom curve) to $v = 0$ (top curve). As in Fig. 4 the gas temperature is shown as a reference, but on a different scale.

information given in Section 2, the pre-shock fractional abundances have been introduced taking into account that the gas in the intergalactic medium before the formation of the first stars has a residual fractional ionization and a fraction of $H_2 \sim 10^{-6}$. Accordingly to the results shown in Coppola et al. (2011b), we assumed this fraction to be in the ground vibrational level. The pre-shock temperature is given by the gas temperature at the value of z at which the calculation is carried out, $T_1 = T(z)$. The post-shock ionization degrees have been calculated according to Saha's equations (equations 3–6) coupled to mass, momentum and energy convervation equations. Including the terms corresponding to hydrogen, helium and deuterium ionization in the energy conservation equation, we obtain a post-shock temperature $\sim 6 \times 10^5$ K.

The chemical composition of the post-shock gas is shown in Fig. 3 as function of time after the shock in units of the Hubble time, $t_H \equiv H_0^{-1} = 4.59 \times 10^{17}$ s. The latter is computed using the most recent value of the Hubble constant H_0 from Planck Collaboration XIII (2015). Starting from an initially ionized atomic gas, the formation of several molecules and of the negatively charged hydrogen ion is observed to occur at $t/t_H \sim 0.003$ following the recombination epoch.

Figs 4 and 5 show the evolution of the populations of the vibrational manifolds of H_2 and H_2^+, while Figs 6 and 7 show the non-equilibrium distributions of vibrational levels of H_2 and H_2^+ compared to the Boltzmann distributions at the gas temperature of the corresponding times in the evolution of the shock. As in the case of the primordial Universe chemistry, it is possible to see two steps in the evolution of the fractional abundance of H_2: the former is related to the formation through the charge transfer between H_2^+ and H at $\sim 10^{-3}$ and $\sim 10^{-2}$ Hubble times, corresponding to a gas temperature between 10^6 and 20 000 K. Indeed, a rise in the H_2^+ fractional abundance can be seen even at slightly earlier phases. The second step is due to the H^- channel. Note the drop of the fractional abundances of the vibrational levels population for levels higher than $v = 9$. This is due to the characteristic endothermicity of the associative detachment process for highly excited levels, as pointed out in the case of the early Universe chemistry by Coppola et al. (2011a). The suprathermal tails arise because of recombination processes: starting from an initial phase of underpopulated levels, an increased production of higher excited levels can be noted. The temperature associated with the first vibrational transition is significantly smaller than the temperature associated with the tail of the distribution.

Concerning the H_2^+ vibrational level population it can be noticed that the formation channel via HeH^+ is responsible for the bumps present at later times in the shock evolution ($t/t_H > 4 \times 10^{-3}$). In the present simulation, we assume that only the first three levels of the molecular hydrogen cation are formed via HeH^+ and that they are produced with the same specific rate. A detailed state-to-state calculation could in principle discriminate among the levels and provide a more accurate description for the chemical kinetics; for this, new data are needed.

As a comparison with previous H_2 cooling calculations, the non-equilibrium cooling function and the fit provided by Glover & Abel (2008) and Glover (2015) are compared in Fig. 8. The non-equilibrium cooling function has been calculated adopting the

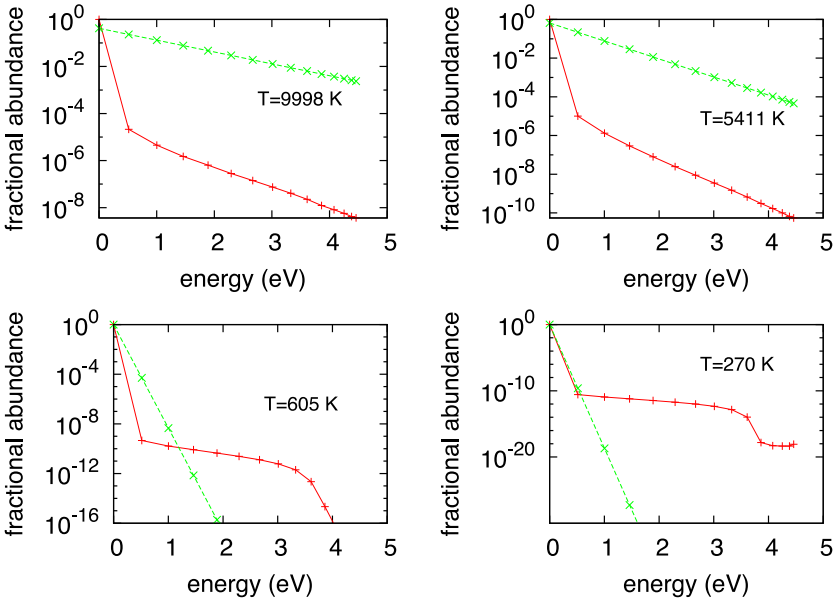

Figure 6. Vibrational distribution function of H_2 at different gas temperatures, corresponding to different times of the evolution (solid red curves). The equilibrium vibrational distribution function at the gas temperature at the same time of the time evolution of the shock is also shown (dotted green lines with crosses). At longer times from the initial shock (i.e. at lower gas temperatures), non-equilibrium features still characterize the shape of the distribution; in particular, suprathermal tail can be noticed due to recombination processes occurring in the system.

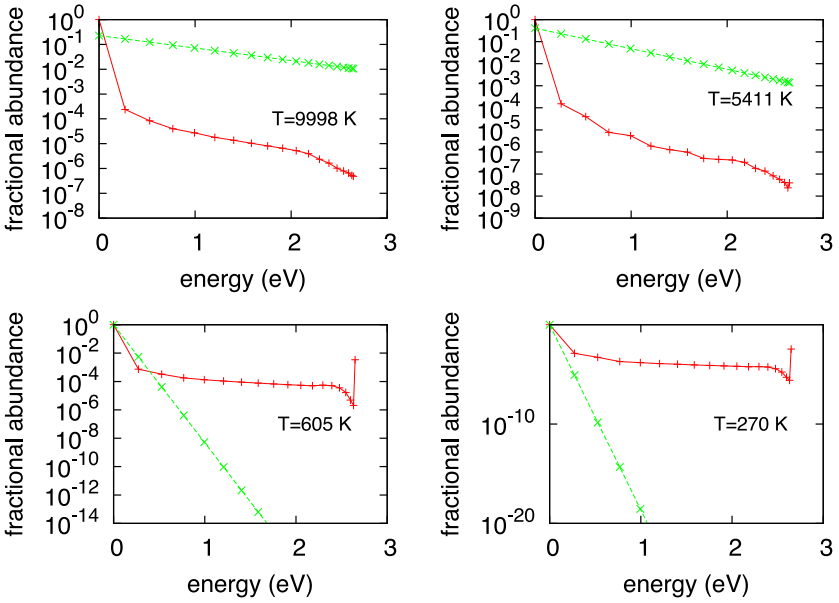

Figure 7. As Fig. 6 but for H_2^+.

usual expressions (Tiné, Lepp & Dalgarno 1998; Omukai 2000):

$$\Lambda = \sum_{E_{v_i,j_i} > E_{v_f,j_f}} n_{v_i,j_i} A_{(v_i,j_i)\rightarrow(v_f,j_f)} (E_{v_i,j_i} - E_{v_f,j_f}), \quad (32)$$

where n_{v_i,j_i} is the density of the initial roto-vibrational state, $A_{(v_i,j_i)\rightarrow(v_f,j_f)}$ is the spontaneous transition probability between an initial (v_i, j_i) roto-vibrational state to a final (v_f, j_f) one, E_{v_i,j_i} and E_{v_f,j_f} the energies of the initial and final state, respectively. The cooling function calculated according to this procedure cannot probe any rotational non-equilibrium effects. However, since a complete set of rotationally resolved reaction rates for the most relevant processes involving H_2 is not available, we assumed that the populations of the rotational levels follow a Boltzmann distribution at the gas temperature. This is equivalent to considering only the vibrational 'component' of the H_2–H cooling rate. This approximation is valid only at high temperatures: above ∼2000 K, the vibrational cooling function and the H_2 cooling function by Glover & Abel (2008) differ for at most a factor 3.5. The comparison with the fit provided by Glover & Abel (2008) can be significant only during these first phases of the post-shock, when the low-density limit is satisfied and the gas temperature is high enough that the vibrational transitions are expected to play a more relevant role than the rotational ones. However, the assumed LTE population for the rotational transitions is questionable at these density regimes. For

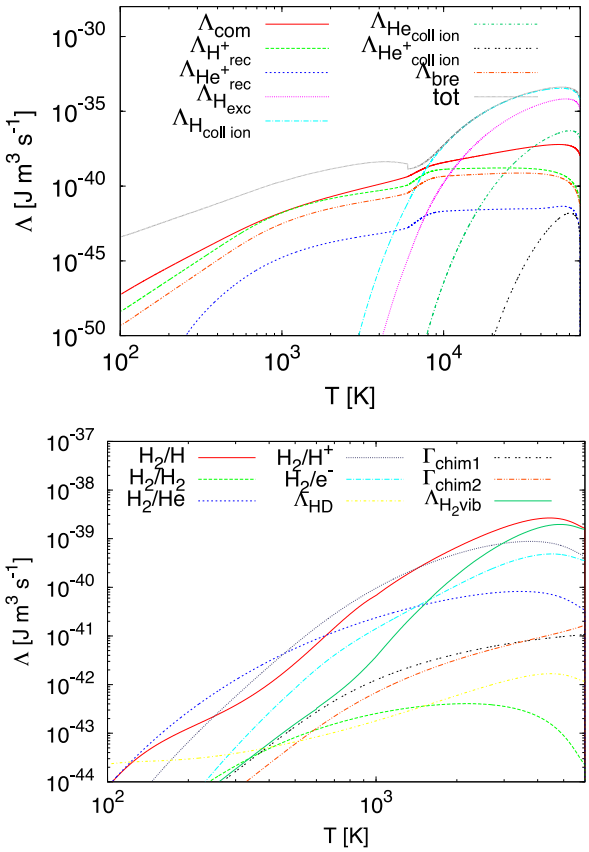

Figure 8. Cooling functions for the post-shock gas. Top panel: atomic, ionic, free-electrons (Compton and Bremsstrahlung) and H^+/He^+/He^{++} cooling functions. Bottom panel: molecular contributions; namely, the H_2 cooling functions for collisions with H, H_2, He (Glover & Abel 2008), H^+ and e^- (Glover 2015, the last four contributions have been included in the equation for the evolution of the temperature); H_2 non-equilibrium vibrational cooling function (see the text for the details) and HD cooling function by Lipovka et al. (2005). The chemical contribution to the heating due to the associative detachment of H^- (Γ_1) and H^- formation due to electron attachment (Γ_2) are also reported and included in the model.

this reason, in order to verify the sensitivity of the vibrational cooling function on several assumptions on the rotational distribution, we have run the simulation with different hypothesis: ground state approximation (where only the fundamental rotational level j=0 of each vibrational level v is considered) and LTE rotational distribution with temperature smaller than the effective gas temperature, in order to simulate the expected subthermal distribution at low densities. The results are shown in Fig. 9 and they suggest that, as a first approximation, the effects on the vibrational cooling function (and eventually on the chemistry) are negligible.

In order to model the non-equilibrium cooling it is useful to compute the excitation temperature of the lowest transition

$$T_{0-1} \equiv \frac{E_1 - E_0}{k_B \ln(n_{H_2,0}/n_{H_2,1})}, \quad (33)$$

where E_1 and E_0 are the energies of the first excited and ground vibrational level and $n_{H_2,1}$ and $n_{H_2,0}$ their abundances. Initially, the excitation temperature T_{0-1} diverges since the H_2 is still forming. In fact, according to the definition given in equation (33) fractional abundances are very small and eventually the logarithm diverges. For this reason, in Fig. 2 the excitation temperature is shown starting from a fixed value of t/t_H when the fractional abundances start

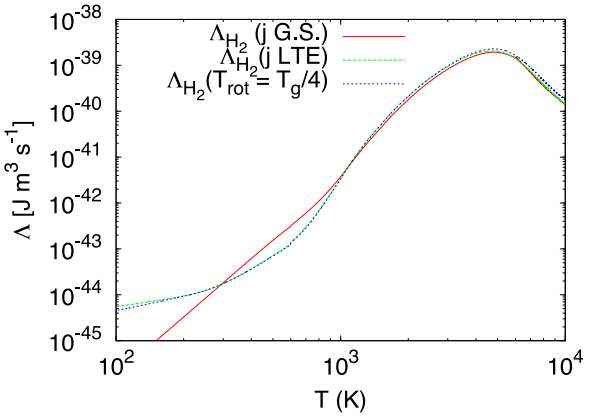

Figure 9. H_2 cooling function: comparison among different approximations for the rotational levels of H_2. Three cases have been reported: (i) LTE at gas temperature (ii) LTE at a gas temperature four times smaller than the gas temperature at each time (iii) ground state (G.S.) approximation.

to be significant. Once H_2 starts to form, the excitation temperature reaches a value higher than the radiation and gas temperatures as shown in Fig. 2. Although the gas temperature changes very rapidly and varies over several orders of magnitude, the excitation temperature T_{0-1} tends rapidly to the final value of few hundreds K. Hence, while the gas and the radiation reach thermal equilibrium, molecular vibration is decoupled as a result of the non-equilibrium patterns in the vibrational distribution.

The state-to-state formation and destruction pathways have been explicitly implemented in the kinetics. This means that the energy deposited in the gas by exothermal chemical processes is explicitly included according to the kinetics itself. However, this energy is not transferred back to the gas and transformed into kinetic energy since the densities at which such heating mechanisms are relevant are far from the present conditions that are limited to $n \leq 10^8$ cm^{-3}.

In order to provide an estimate for the sensitivity of our results to redshift and shock velocity, we have run several models with different initial conditions. The results are shown in Fig. 10 and can be summarized as follows: a change in the redshift z implies a variation of the initial density that eventually produces a shift in time in the fractional abundances, leaving the characteristic time-scales unchanged. On the other hand, a variation on the velocity of the shock affects the time-scales of processes, pushing the recombination to be completed at earlier times for faster shocks. The cases for z = 20, 25 and v_s = 30–50 km s^{-1} are shown in Fig. 10.

4 CONCLUSIONS

We have performed a numerical calculation of the chemical kinetics for a shock-heated gas of primordial composition. Particular attention has been paid to the distribution of the vibrational levels of molecular hydrogen and its cation. Unlike previous studies that assumed vibrational equilibrium for the level population, here we show that this assumption is not always justified. In fact, in our calculations the vibrational level populations are shown to deviate strongly from the equilibrium predictions. The case study considered here is that of a shock wave produced by a primordial Supernova explosion. The results show that H_2 cooling is crucial for lowering the temperature down to ∼200 K when the populations of the vibrational levels of H_2 and H_2^+ molecules are out-of-equilibrium. As for H_2, we find that the vibrational distribution becomes unimportant as long as the temperature exceeds ∼10^3 K. The first excited

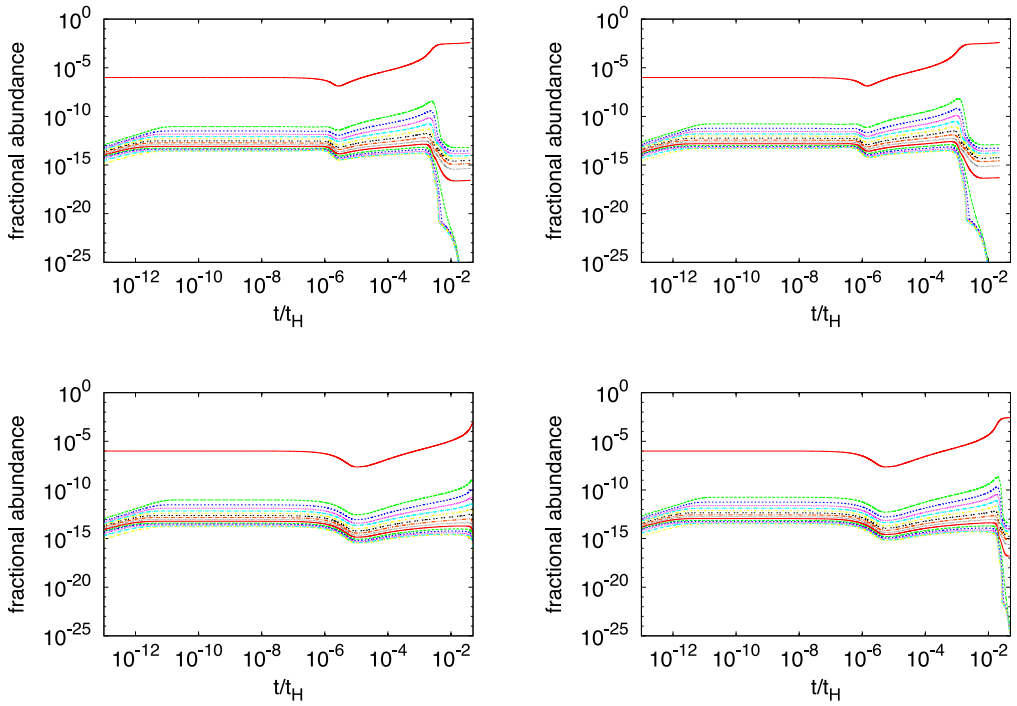

Figure 10. H_2 vibrational level population for different initial condition for redshift z and shock velocity v_s. Top panels, from left to right: standard case ($z = 20$, v_s=50 km s^{-1}), case 1 ($z = 25$, v_s=50 km s^{-1}). Bottom panels, from left to right: case 2 ($z = 20$, v_s=30 km s^{-1}), case 3 ($z = 25$, v_s=30 km s^{-1}). It can be noticed that a change in the redshift z results in a time shit of the fractional abundance as a function of time; on the other hand, a change in the shock velocity affects the typical recombination scales. For this reason in the case of higher shock velocities recombination proceeds slightly faster allowing to reach the freeze-out fractional abundances earlier in time.

vibrational level has been found to be at the equilibrium value for low temperatures, but since the H_2 formation tends to populate the higher vibrational levels, a non-equilibrium distribution is produced for $v \geq 2$.

We plan to extend the present calculations changing the chemical content of the gas allowing for the presence of heavy elements. A rotationally resolved chemical kinetics should also be considered allowing to relax the assumption of rotational equilibrium. In this way we could be able to properly describe any possible non-equilibrium effects on the cooling function, related to the inclusion of a state-to-state approach in the description of molecular systems, especially at low temperature. Moreover, the chemistry of H_2^+ should be updated according to more recent results on the photodissociation and HeH^+ channels (Esposito, Coppola & De Fazio 2015; Vujcic et al. 2015) Finally, optical depth effects may be included for a complete treatment of the post-shock gas in a variety of environments.

ACKNOWLEDGEMENTS

The Authors are grateful to the anonymous referee for the valuable comments suggested. CMC, GM and SL acknowledge financial support of MIUR-PRIN (grant no. 2010ERFKXL). This work has also been partially supported by the FP7 project 'Phys4Entry' – grant agreement no. 242311. CMC is grateful to the CNR-IMIP computing facilities, in particular to Dr Pierpaolo Minelli for technical support. CMC, DG, SL and FP acknowledge the discussions within the international team #272 lead by C. M. Coppola 'EUROPA – Early Universe: Research on Plasma Astrochemistry' at ISSI (International Space Science Institute) in Bern. GM acknowledges partial support from the EPSRC under grant number EP/L015374/1.

REFERENCES

Abel T., Anninos P., Zhang Y., Norman M. L., 1997, New Astron., 2, 181
Anninos P., Zhang Y., Abel T., Norman M. L., 1997, New Astron., 2, 209
Birnboim Y., Keshet U., Hernquist L., 2010, MNRAS, 408, 199
Black J. H., 1981, MNRAS, 197, 553
Cízek M., Horácek J., Domcke W., 1998, J. Phys. B: At. Mol. Opt. Phys., 31, 2571
Coppola C. M., Longo S., Capitelli M., Palla F., Galli D., 2011a, ApJS, 193, 7
Coppola C. M., Lodi L., Tennyson J., 2011b, MNRAS, 415, 487
Dickinson A. S., 2008, J. Phys. B: At. Mol. Opt. Phys., 41, 049801
Esposito F., Capitelli M., 2009, J. Phys. Chem. A, 113, 15307
Esposito F., Coppola C. M., De Fazio D., 2015, J. Phys. Chem. A, 119, 12615
Flower D. R., 1997, J. Phys. B: At. Mol. Opt. Phys., 30, 3009
Flower D. R., Roueff E., 1998, J. Phys. B: At. Mol. Opt. Phys., 31, L955
Galli D., Palla F., 1998, A&A, 335, 403
Galli D., Palla F., 2002, A&A, 50, 1197
Gerlich D., Horning S., 1992, Chem. Rev., 92, 1509
Glover S. C. O., 2015, MNRAS, 451, 2082
Glover S. C. O., Abel T., 2008, MNRAS, 388, 1627
Glover S. C. O., Jappsen A.-K., 2007, ApJ, 666, 1
Glover S. C. O., Savin D. W., 2009, MNRAS, 393, 911
Haiman Z., Rees M. J., Loeb A., 1996, ApJ, 467, 522
Ignjatović L. M., Mihajlov A. A., Srećković V. A., Dimitrijević M. S., 2014, MNRAS, 441, 1504
Johnson J. L., Bromm V., 2006, MNRAS, 366, 247
Jurek M., Spirko V., Kraemer W., 1995, Chem. Phys., 193, 287
Kreckel H., Bruhns H., Cízek M., Glover S. C. O., Miller K. A., Urbain X., Savin D. W., 2010, Science, 329, 69
Krstic P. S., 2002, Phys. Rev. A, 66, 042717
Krstic P. S., Schultz D. R., Janev R. K., 2002, Phys. Scr., 2002, 61
Lepp S., Stancil P. C., Dalgarno A., 2002, J. Phys. B: At. Mol. Opt. Phys., 35, 57

Linder F., Janev R., Botero J., 1995, in Janev R., ed., Atomic and Molecular Processes in Fusion Edge Plasmas. Springer-Verlag, Berlin, p. 397
Lipovka A., Núñez López R., Avila-Reese V., 2005, MNRAS, 361, 850
McCall B. J. et al., 2004, Phys. Rev. A, 70, 052716
Machida M. N., Tomisaka K., Nakamura F., Fujimoto M. Y., 2005, ApJ, 622, 39
Mihajlov A. A., Ignjatović L. M., Sakan N. M., Dimitrijević M. S., 2007, A&A, 469, 749
Miller S., Stallard T., Melin H., Tennyson J., 2010, Faraday Discuss., 147, 283
Motapon O., Tamo F. O. W., Urbain X., Schneider I. F., 2008, Phys. Rev. A, 77, 052711
Motapon O. et al., 2014, Phys. Rev. A, 90, 012706
Omukai K., 2000, ApJ, 534, 809
Planck Collaboration XIII, 2015, preprint (arXiv:1502.01589)
Savin D. W., 2002, ApJ, 566, 599
Schatz G. C., Badenhoop J. K., Eaker C. W., 1987, Int. J. Quantum Chem., 31, 57
Schleicher D. R. G., Galli D., Palla F., Camenzind M., Klessen R. S., Bartelmann M., Glover S. C. O., 2008, A&A, 490, 521
Shapiro P. R., Kang H., 1987, ApJ, 318, 32
Shchekinov Y. A., Vasiliev E. O., 2006, MNRAS, 368, 454
Sidhu K. S., Miller S., Tennyson J., 1992, A&A, 255, 453
Stancil P. C., Lepp S., Dalgarno A., 1998, ApJ, 509, 1
Strömholm C. et al., 1995, Phys. Rev. A, 52, R4320
Takagi H., 2005, J. Phys.: Conf. Ser., 4, 155
Takizawa M., Mineshige S., 1998, ApJ, 499, 82
Theard L. P., Huntress W. T., 1974, J. Chem. Phys., 60, 2840
Tiné S., Lepp S., Dalgarno A., 1998, Mem. Soc.à Astron. Ital., 69, 345
Vujcic V., Jevremovic D., Mihajlov A. A., Ignjatovic Lj. M., Sreckovic V. A., Dimitrijevic M. S., Malovic M., 2015, JApA, 36, 693
Wolniewicz L., Simbotin I., Dalgarno A., 1998, ApJS, 115, 293
Zygelman B., Dalgarno A., Kimura M., Lane N. F., 1989, Phys. Rev. A, 40, 2340
Zygelman B., Stancil P. C., Dalgarno A., 1998, ApJ, 508, 151

APPENDIX A: TABLES

A list of the processes considered in this work can be found in the following tables, together with analytical fits of the rate coefficients and the references from which the data have been derived. For clarity, we have defined $T_0 = 11604.5$ K, the temperature corresponding to 1 eV, and denoted the gas temperature and the radiation temperature (both in K) as T and T_r, respectively. ln and $\log_1 0$ represent the base e and base 10 logarithms.

Table A1. Chemical reactions and rate coefficients.

Chemical process	Rate coefficient ($m^3\ s^{-1}$ or s^{-1})	Ref.
1) $H + e^- \rightarrow H^- + h\nu$	$1.4 \times 10^{-24} T^{0.928} \exp(T/16200)$	Galli & Palla (1998)
2) $H^- + e^- \rightarrow H + 2e^-$	$1.27 \times 10^{-17} T^{1/2} \exp(-157809.1/T)(1 + T_5^{1/2})^{-1}$	Black (1981)
		Haiman, Rees & Loeb (1996)
3) $H^- + H \rightarrow 2H + e^-$	for $T > 1160.45$	Abel et al. (1997)
	$10^{-6} \exp[-20.37260896 + 1.13944933 \ln(T/T_0) +$	
	$-0.14210135 \ln(T/T_0)^2 +$	
	$+8.4644554 \times 10^{-3} \ln(T/T_0)^3 +$	
	$-1.4327641 \times 10^{-3} \ln(T/T_0)^4 +$	
	$+2.0122503 \times 10^{-4} \ln(T/T_0)^5 +$	
	$+8.6639632 \times 10^{-5} \ln(T/T_0)^6 +$	
	$-2.5850097 \times 10^{-5} \ln(T/T_0)^7 +$	
	$+2.4555012 \times 10^{-6} \ln(T/T_0)^8 +$	
	$-8.0683825 \times 10^{-8} \ln(T/T_0)^9]$	
	for $T < 1160.45$: $2.5634 \times 10^{-15} \times T^{1.78186}$	
4) $H^- + H^+ \rightarrow 2H$	$1.4 \times 10^{-13} (T/300)^{-0.487} \exp(T/29300)$	Schleicher et al. (2008)
5) $H^- + h\nu \rightarrow H + e^-$	$0.01\ T_r^{2.13} \exp(-8823/T_r)$	Coppola et al. (2011a)
6) $D^- + h\nu \rightarrow D + e^-$	as (5)	Coppola et al. (2011a)
7) $HD^+ + h\nu \rightarrow D + H^+$	$0.5 \times 1.63 \times 10^7 \exp(-32400/T_r)$	Galli & Palla (1998)
8) $HD^+ + h\nu \rightarrow H + D^+$	$0.5 \times 1.63 \times 10^7 \exp(-32400/T_r)$	Galli & Palla (1998)
9) $HD^+ + h\nu \rightarrow H^+ + D^+ + e$	$9 \times 10^1\ T_r^{1.48} \exp(-335000/T_r)$	Galli & Palla (1998)
10) $H + e^- \rightarrow H^+ + 2e^-$	$10^{-6} \exp[-32.71396786 + 13.536556 \ln(T/T_0) +$	Abel et al. (1997)
	$-5.73932875 \ln(T/T_0)^2 +$	
	$+1.56315498 \ln(T/T_0)^3 +$	
	$-0.2877056 \ln(T/T_0)^4 +$	
	$+3.48255977 \times 10^{-2} \ln(T/T_0)^5 +$	
	$-2.63197617 \times 10^{-3} \ln(T/T_0)^6 +$	
	$+1.11954395 \times 10^{-4} \ln(T/T_0)^7 +$	
	$-2.03914985 \times 10^{-2} \ln(T/T_0)^8]$	
11) $H^+ + e^- \rightarrow H + h\nu$	$2.753 \times 10^{-20} (315614/T)^{1.5} (1 + (115188/T)^{0.407})^{-2.242}$	Glover & Savin (2009)
12) $He^{++} + e^- \rightarrow He^+ + h\nu$	$5.506 \times 10^{-20} (1262456/T)^{1.5} (1 + (460752/T)^{0.407})^{-2.242}$	Glover & Abel (2008)
13) $He^+ + e^- \rightarrow He + h\nu$	$10^{-17} T^{-0.5}\ \cdot$	Glover & Abel (2008)
	$(11.19 - 1.676(\log_{10} T) - 0.2852(\log_{10} T)^2 + 0.04433(\log_{10} T)^3) +$	
	$+ (1.9 \times 10^{-9} T^{-1.5} \exp(-473421/T))(1 + 0.3 \exp(-94684/T))$	

Table A1. – *continued*

Chemical process	Rate coefficient ($m^3\ s^{-1}$ or s^{-1})	Ref.
14) $HD + h\nu \rightarrow HD^+ + e^-$	$2.9 \times 10^2 T_r^{1.56} \exp(-178500/T_r)$	Galli & Palla (1998)
15) $D^+ + e^- \rightarrow D + h\nu$	as (11)	
16) $D^+ + H \rightarrow D + H^+$	$2.06 \times 10^{-16} T^{0.396} \exp(-33/T) + 2.03 \times 10^{-15} T^{-0.332}$	Savin (2002)
17) $H^+ + D \rightarrow H + D^+$	$2 \times 10^{-16} T^{0.402} \exp(-37.1/T) - 3.31 \times 10^{-23} T^{1.48}$	Savin (2002)
18) $D + H \rightarrow HD + h\nu$	$10^{-32}[2.259 - 0.6(T/1000)^{0.5} + 0.101(T/1000)^{-1.5}$ $-0.01535(T/1000)^{-2} + 5.3 \times 10^{-5}(T/1000)^{-3}]$	Dickinson (2008)
19) $HD^+ + H \rightarrow HD + H^+$	6.4×10^{-16}	Stancil, Lepp & Dalgarno (1998)
20) $D + H^+ \rightarrow HD^+ + h\nu$	$10^{-6} \mathrm{dex}[-19.38 - 1.523 \log_{10} T +$ $+1.118(\log_{10} T)^2 - 0.1269(\log_{10} T)^3]$	Galli & Palla (1998)
21) $H + D^+ \rightarrow HD^+ + h\nu$	as (19)	
22) $HD^+ + e^- \rightarrow D + H$	$7.2 \times 10^{-14} T^{-0.5}$	Strömholm et al. (1995)
23) $D + e^- \rightarrow D^- + h\nu$	$3 \times 10^{-22} (T/300)^{0.95} \exp(-T/9320)$	Stancil et al. (1998)
24) $D^+ + D^- \rightarrow 2D$	$1.96 \times 10^{-13} (T/300)^{-0.487} \exp(T/29300)$	Lepp, Stancil & Dalgarno (2002)
25) $H^+ + D^- \rightarrow D + H$	$1.61 \times 10^{-13} (T/300)^{-0.487} \exp(T/29300)$	Lepp et al. (2002)
26) $H^- + D \rightarrow H + D^-$	$6.4 \times 10^{-15} (T/300)^{0.41}$	Stancil et al. (1998)
27) $D^- + H \rightarrow D + H^-$	as (25)	
28) $D^- + H \rightarrow HD + e^-$	$1.5 \times 10^{-21} (T/300)^{-0.1}$	Stancil et al. (1998)
29) $D + H^- \rightarrow HD + e^-$	as (23)	Schleicher et al. (2008)
30) $H^- + D^+ \rightarrow D + H$	$1.61 \times 10^{-13} (T/300)^{-0.487} \exp(T/29300)$	Lepp et al. (2002)
31) $D + H_2 \rightarrow HD + H$	$T < 250$ K: $1.69 \times 10^{-16} \exp(-4680/T + 198800/T^2)$	Galli & Palla (2002)
	$T > 250$ K: $9 \times 10^{-17} \exp(-3876/T)$	Galli & Palla (1998)
32) $D^+ + H_2 \rightarrow HD + H^+$	$10^{-15}(0.417 + 0.846 \log_{10} - 0.137 \log_{10}^2)$	Galli & Palla (2002)
33) $HD + H \rightarrow D + H_2$	$T < 200$ K: $5.25 \times 10^{-17} \exp(-4430/T + 173900/T^2)$	Galli & Palla (2002)
	$T > 200$ K: $3.2 \times 10^{-17} \exp(-3624/T)$	Galli & Palla (1998)
34) $HD + H^+ \rightarrow D^+ + H_2$	$1.1 \times 10^{-15} \exp(-488/T)$	Galli & Palla (2002)
35) $He + H^+ \rightarrow He^+ + H$	$T > 10^4$ K: $4 \times 10^{-43} T^{4.74}$	Galli & Palla (1998)
	$T < 10^4$ K: $1.26 \times 10^{-15} T^{-0.75} \exp(-127500/T)$	Glover & Jappsen (2007)
36) $H + He^+ \rightarrow H^+ + He$	$1.25 \times 10^{-21} (T/300)^{0.25}$	Zygelman et al. (1989)
37) $He + H^+ \rightarrow HeH^+ + h\nu$	$8 \times 10^{-26} (T/300)^{-0.24} \exp(-T/4000)$	Stancil et al. (1998)
38) $He + H^+ + h\nu \rightarrow HeH^+ + h\nu$	$3.2 \times 10^{-26}[T^{1.8}/(1 + 0.1T^{2.04})] \times$ $\times \exp(-T/4000)(1 + 2 \times 10^{-4} T_r^{1.1})$	Jurek, Spirko & Kraemer (1995)
		Zygelman et al. (1998)
39) $He + H_2^+ \rightarrow HeH^+ + H$	$3 \times 10^{-16} \exp(-6717/T)$	Galli & Palla (1998)
40) $He^+ + H \rightarrow HeH^+ + h\nu$	$4.16 \times 10^{-22} T^{-0.37} \exp(-T/87600)$	Stancil et al. (1998)
41) $HeH^+ + H \rightarrow He + H_2^+$	$0.69 \times 10^{-15} (T/300)^{0.13} \exp(-T/33100)$	Linder, Janev & Botero (1995)
42) $HeH^+ + e \rightarrow He + H$	$3 \times 10^{-14} (T/300)^{-0.47}$	Stancil et al. (1998)
43) $HeH^+ + h\nu \rightarrow He + H^+$	$220 \times T_r^{0.9} \exp(-22740/T_r)$	Jurek et al. (1995)
44) $HeH^+ + h\nu \rightarrow H + He^+$	$7.8 \times 10^3 T_r^{1.2} \exp^{-240000/T_r}$	Galli & Palla (1998)
45) $H_2 + H^+ \rightarrow H_3^+ + h\nu$	10^{-22}	Gerlich & Horning (1992)
46) $H_3^+ + e \rightarrow H_2 + H$	$0.34 \times (1.27 \times 10^{-12} T^{-0.48} - 1.3 \times 10^{-14})$	McCall et al. (2004)
47) $H_3^+ + e \rightarrow H + H + H$	$0.66 \times (1.27 \times 10^{-12} T^{-0.48} - 1.3 \times 10^{-14})$	McCall et al. (2004)
48) $H_2^+ + H_2 \rightarrow H_3^+ + H$	2×10^{-15}	Theard & Huntress (1974)
49) $H_3^+ + H \rightarrow H_2^+ + H_2$	$7.7 \times 10^{-15} \exp(-17560/T)$	Sidhu, Miller & Tennyson (1992)
50) $H_2 + He^+ \rightarrow He + H + H^+$	$2.7 \times 10^{-14} T^{-1.27} \exp(-43000/T)$	Glover & Abel (2008)
51) $H_2 + He^+ \rightarrow H_2^+ + He$	$3.7 \times 10^{-20} \exp(35/T)$	Glover & Abel (2008)
52) $He + e \rightarrow He^+ + e + e$	$2.38 \times 10^{-17} T^{0.5} \exp(-285335.4/T)$	Black (1981)
	$\times(1 + \sqrt{T/10^5})^{-1}$	Haiman et al. (1996)
53) $He^+ + e \rightarrow He^{++} + e + e$	$5.68 \times 10^{-18} T^{0.5} \exp(-631515/T)$	Black (1981)
	$\times(1 + \sqrt{T/10^5})^{-1}$	Haiman et al. (1996)

Table A2. Molecular processes: vibrationally resolved reactions. All data for these processes are from Coppola et al. (2011a).

	Chemical process
1	$H + H_2(v) \rightarrow H + H_2(v')$
2	$H + H^- \rightarrow H_2 + e^-$
3	$H + H^+ \rightarrow H_2^+ + h\nu$
4	$H_2^+(v) + H \rightarrow H_2(v') + H^+$
5	$H_2(v) + H^+ \rightarrow H_2^+(v') + H$
6	$H + H_2^+(v) \rightarrow H + H_2^+(v')$
7	$H^+ + H_2(v) \rightarrow H^+ + H_2(v')$
8	$H + H_2(v) \rightarrow H + H_2(v')$
9	$H^+ + H_2(v) \rightarrow H + H + H^+$
10	$H_2(v) + h\nu \rightarrow H_2^+(v') + e^-$
11	$H_2^+(v) + h\nu \rightarrow H + H^+$
12	$H_2(v) + h\nu \rightarrow H + H$
13	$H_2^+(v) + e^- \rightarrow H + H$
14	$H_2(v) + e^- \rightarrow H^- + H$
15	$H_2(v) + e^- \rightarrow H_2^* \rightarrow H_2(v') + e^- + h\nu$
16	$H_2(v) \rightarrow H_2(v') + h\nu$
17	$H_2^+(v) \rightarrow H_2^+(v') + h\nu$
18	$H + H_2(v) \rightarrow H + H + H$

Table A3. Cooling functions included in the thermal evolution. The symbol T_n stands for $T/10^n$.

	Process	J m^3 s^{-1} or J s^{-1}	Reference
Atomic processes			
	-collisional excitation		
	H	$7.50 \times 10^{-32} \exp(-118348/T)(1 + T_5^{1/2})^{-1}$	Anninos et al. (1997)
	-collisional ionization		
	H	$1.27 \times 10^{-34} T^{1/2} \exp(-157809.1/T)(1 + T_5^{1/2})^{-1}$	Haiman et al. (1996)
	He	$9.38 \times 10^{-35} T^{1/2} \exp(-285335.4/T)(1 + T_5^{1/2})^{-1}$	Haiman et al. (1996)
	He	$4.95 \times 10^{-35} T^{1/2} \exp(-631515./T)(1 + T_5^{1/2})^{-1}$	Haiman et al. (1996)
	-bremsstrahlung	$1.42 \times 10^{-40} T^{1/2}[1.10 + 0.34$	
		$\exp(-(5.50 - \log_{10} T)^2/3)]$	Haiman et al. (1996)
	-Compton cooling/heating	$1.017 \times 10^{-44} T_r^4 (T - T_r)$	Anninos et al. (1997)
	-recombination		
	H^+	$8.70 \times 10^{-40} T^{1/2} T_3^{-0.2}[(1 + T_6^{0.7})^{-1}]$	Haiman et al. (1996)
	He^+	$1.55 \times 10^{-39} T^{0.3647}$	
		$+1.24 \times 10^{-26} T^{-1.5}(1 + 0.3\exp(-94000/T))$	
		$\exp(-470000/T)$	Haiman et al. (1996)
	He^{++}	$3.48 \times 10^{-39} T^{1/2} T_3^{-0.2}(1 + T_6^{0.7})^{-1}$	Haiman et al. (1996)
	-e^- attachment to H		(calculated using reaction rate 1)
Molecular processes			
	collisional cooling		
	H_2/H	see reference	Glover & Abel (2008)
	H_2/H_2	//	Glover & Abel (2008)
	H_2/He	//	Glover & Abel (2008)
	H_2/H^+	//	Glover (2015)
	H_2/e^-	//	Glover (2015)
	HD cooling	$\Lambda(T, n)$	Lipovka et al. (2005)
Heating process			
	H^- channel for H_2 formation	vibrationally resolved (equation 31)	cross-sections by Cízek et al. (1998)

This paper has been typeset from a TEX/LATEX file prepared by the author.